



HAL
open science

The light intensity at which cells are grown controls the type of peripheral light-harvesting complexes that are assembled in a purple photosynthetic bacterium

Tatas Hardo Panintingjati Brotosudarmo, Aaron M. Collins, Andrew Gall, Aleksander W. Roszak, Alastair T. Gardiner, Robert E Blankenship, Richard John Cogdell

► To cite this version:

Tatas Hardo Panintingjati Brotosudarmo, Aaron M. Collins, Andrew Gall, Aleksander W. Roszak, Alastair T. Gardiner, et al.. The light intensity at which cells are grown controls the type of peripheral light-harvesting complexes that are assembled in a purple photosynthetic bacterium. *Biochemical Journal*, 2011, 440 (1), pp.51-61. 10.1042/BJ20110575 . hal-00642834

HAL Id: hal-00642834

<https://hal.science/hal-00642834>

Submitted on 19 Nov 2011

HAL is a multi-disciplinary open access archive for the deposit and dissemination of scientific research documents, whether they are published or not. The documents may come from teaching and research institutions in France or abroad, or from public or private research centers.

L'archive ouverte pluridisciplinaire **HAL**, est destinée au dépôt et à la diffusion de documents scientifiques de niveau recherche, publiés ou non, émanant des établissements d'enseignement et de recherche français ou étrangers, des laboratoires publics ou privés.

The light intensity at which cells are grown controls the type of peripheral light-harvesting complexes that are assembled in a purple photosynthetic bacterium

Tatas H.P. Brotosudarmo^{*, ||}, Aaron M. Collins^{†, ¶}, Andrew Gall[‡], Aleksander W. Roszak[§], Alastair T. Gardiner^{*}, Robert E. Blankenship[†] and Richard J. Cogdell^{*}

^{*} Institute of Molecular Cell and System Biology, College of Medical, Veterinary and Life Sciences, University of Glasgow, Glasgow Biomedical Research Building, 120 University Place, G12 8TA, UK

[†] Departments of Biology and Chemistry, Washington University in St. Louis, Campus Box 1137, 1 Brookings Dr., St. Louis, MO 63130, USA

[‡] CEA-Saclay, Institute de Biologie et Technologies de Saclay et CNRS/URA2096, 91191 Gif-sur-Yvette, France

[§] Department of Chemistry, WestChem, University of Glasgow, Glasgow Biomedical Research Building, 120 University Place, G12 8TA, UK

^{||} Present address: Ma Chung Research Center for Photosynthetic Pigments (MRCPP), Ma Chung University, Jl. Villa Puncak Tidar N01, Malang 65151, Indonesia

[¶] Present address: Bioenergy and Defense Technology, Sandia National Laboratories, Albuquerque, NM 87185, USA.

Corresponding Author: Prof. Richard J. Cogdell, Tel: +44-141-330-4232, Fax: +44-141-330-3779, Email: richard.cogdell@glasgow.ac.uk

Running title: LH2 *Rps. palustris* Quaternary Structure

Keywords: Purple photosynthetic bacteria, *Rhodospseudomonas palustris*, light harvesting complexes, X-ray crystallography, *puc* genes.

Synopsis

The differing composition of peripheral light harvesting complexes (LH2) present in *Rhodospseudomonas (Rps.) palustris* 2.1.6 have been investigated when cells are grown at progressively decreasing light intensity. Detailed analysis of their absorption spectra reveals that there must be more than two types of LH2 complexes present. Purified high-light (HL) and low-light (LL) LH2 complexes have mixed apoprotein compositions. The HL complexes contain PucAB_a and PucAB_b apoproteins. The LL complexes contain PucAB_a, PucAB_d and PucB_b-only apoproteins. This mixed apoprotein composition can explain their resonance Raman spectra. Crystallographic studies and molecular sieve chromatography suggest that both the HL and the LL complexes are nonameric.

Introduction

Purple bacterial photosynthesis begins when solar energy is absorbed by the light harvesting (LH) complexes. The resulting excitation energy is then funneled to reaction centres (RCs), where charge separation occurs [1]. Most species of purple bacteria have two types of LH complexes: core complexes (LH1) and peripheral complexes (LH2). These complexes are modular with each individual module constructed from pairs of short (50-60 amino acids), very hydrophobic polypeptides called α and β . The LH1 complex from *Rps. palustris*, for example, consists of 15 such α/β -polypeptide modules that are oligomerised to surround the RC [2]. Each module binds two bacteriochlorophyll *a* (Bchl *a*) molecules and one carotenoid (Car) molecule. The Bchl *a* molecules are strongly coupled, giving rise to the intense Q_y absorption band at ~ 875 nm. In the case of the LH2 complex from *Rps. acidophila* strain 10050 each module binds three Bchl *a* molecules and one Car [3, 4, 5]. Nine such modules are arranged circularly to form a single LH2 complex. The α -polypeptide is located inside the ring and the β -polypeptide is on the outside. Nine monomeric Bchl *a* molecules have their bacteriochlorin macrocycles oriented parallel to the plane of the membrane and absorb the light with a near infrared (NIR) absorption maximum at ~ 800 nm. These are called the B800 Bchl *a* molecules. These B800 Bchls are separated, centre-to-centre, by 2.1 nm and are considered monomeric. A further eighteen Bchl *a* molecules have their bacteriochlorin macrocycles oriented perpendicular to the membrane plane. They are responsible for the absorption band at about 850 nm. The macrocycles of the B850 Bchl *a* molecules sit very close to each other, ~ 0.9 nm, and are strongly exciton coupled. In case of *Phs. molischianum* the LH2 complexes are octamers [6].

In some species of purple bacteria, such as *Rps. acidophila* 7050 and 7750 or *Rps. palustris*, the Q_y absorption bands of the Bchl in the LH2 complexes can vary depending on the growth conditions. When *Rps. acidophila* strains 7750 and 7050 are grown under low-light conditions, a different type of LH2 complex is formed with the Q_y absorption bands at 800 and 820 nm rather than at 800 and 850 nm. This different type of LH2 has been called both LH3 and B800-820 LH2 [5, 7, 8]. The ability to change the type of LH2 in response to growth at different light intensities is related to the presence of multiple α/β -polypeptides, which are encoded (in case of *Rps. acidophila*) by at least four different α/β -apoprotein gene pairs (called the *pucBA* genes) [9, 10]. When cells of *Rps. palustris* strain 2.1.6 are grown at high-light (HL) intensity they synthesise a standard LH2 complex with the Q_y absorption bands of Bchl *a* at 800 and 850 nm. At low-light intensity *Rps. palustris* strain 2.1.6 replaces the standard HL LH2 (B800-850) with LL LH2 (B800-low-850) complex [11-15]. Again, this ability to adapt and to synthesise LH2 complexes with different NIR absorption spectra is related to the presence of multiple genes encoding LH2 α/β -polypeptides [16, 17]. The complete genome of *Rps. palustris* has been sequenced [18]. There are five different *pucBA* genes present in the *Rps. palustris* genome (*pucBA_a*, *b*, *c*, *d* and *e*) and their expression is regulated by both light intensity and light colour [18, 19].

In a previous study Hartigan *et al.* described the isolation of yet a different type of LH2 from the low-light grown *Rps. palustris* 2.1.6. [20]. This complex, called by the authors LH4, has an unusual absorption spectrum in the NIR showing only a broad band at ~ 800 nm. The LH4 complex has polypeptides that are encoded by *pucB_d* and *pucA_d* [21]. The LH4 complex has been crystallised and low-resolution diffraction data (7.5\AA) has been collected for these crystals allowing a 7.5\AA -model based on this data to be described [20]. This model suggests that the complex is octameric and that each α/β -apoprotein pair binds an extra Bchl *a* relative

to three Bchl *a*s found in the LH2 from *Rps. acidophila*. An AFM study of LL membranes from *Rps. palustris* also suggested that this LH2 is predominantly octameric [22].

The structures of the HL and LL LH2 complexes could potentially be more complicated than has been generally assumed [12, 18, 23]. Given the profusion of *pucBA* genes, the question arises as to whether the LH2 complexes in *Rps. palustris* consist of rings where each ring is homogeneous, containing only one type of α/β -apoprotein, with the spectroscopic variation due to mixtures of different types of rings, or alternatively can rings be heterogeneous, having mixtures of α/β -apoprotein types within a single LH2 ring. In the later case resultant spectroscopic properties will then depend on the compositions of these mixtures. This has been partially addressed using a range of spectroscopic techniques, which have included electronic absorption, circular dichroism (CD), fluorescence and resonance Raman studies on ensembles [11-15, 24]. It was hypothesised that in the LL LH2 complexes, due to the unique excitation wavelength dependency on the Raman spectrum in the high-frequency Bchl *a* carbonyl region, and the inability to isolate a native B800-820 complex, that rings containing multiple α -apoproteins are present [25]. Quite recently, we have investigated the properties of the LL LH2 using single-molecule spectroscopy [26]. The single-molecule spectra for LL LH2 could only be satisfactorily explained by assuming the presence of a nonameric LH2 ring with a mixture of both B850-like and B820-like site energies [26]. As the B850-like and B820-like Bchls are associated with different apoproteins the spectra could only be explained by assuming the presence of rings with a heterogeneous apoprotein composition. The heterogeneity concept from single-molecule spectroscopy was also supported by femtosecond transient absorption spectroscopy, where high-energy exciton states were found in the regions of both 820 and 850 nm [27]. In this paper, we describe a detailed biochemical characterisation of the LH2 complexes from *Rps. palustris*. We set out to investigate whether there are in fact more than two types of LH2 and, if so, what are their quaternary structures.

Experimental

Cells of *Rps. palustris* strain 2.1.6. were grown anaerobically in C-succinate media [28] at 30°C between rows of incandescent bulbs [25]. In this study, cultures were also placed at different distances away from a single bulb so that the intensity of light illuminating the cell culture could be varied from 220 lx, 90 lx, 20 lx, 10 lx, 6.5 lx to 5.5 lx. In the results section, these light intensities have been called high-light (HL), low-light intermediate 1 (LL1), low-light intermediate 2 (LL2), low-light (LL), far low-light (FLL1) and extreme low-light (FLL2) respectively. To minimise any self-shading, cells were regularly transferred into fresh media to ensure a continual low culture optical density ($OD_{850} = 0.5 \text{ cm}^{-1}$). Cells were harvested by centrifugation (relative centrifugal field, $r_{AV} = 1,248 \text{ g}$, 30 min) and resuspended in 20 mM MES buffer pH 6.8 (Sigma-Aldrich) containing 100 mM KCl. The harvested cells were ruptured by 3 passages through a French Press (950 psi) in the presence of a little DNAase and $MgCl_2$ and the membrane fraction pelleted by centrifugation at $r_{AV} = 184,000 \text{ g}$ for 2 h. The membrane pellet was resuspended and homogenised in 20 mM Tris-HCl pH 8.0 (Fisher Scientific) and the concentration adjusted to give an absorption at 850 nm of 70 cm^{-1} . The membranes were then solubilised by the slow, drop-wise addition of lauryldimethylamine N-oxide (LDAO) (Fluka) to 1% (v/v) final concentration. After stirring for 30 min in the dark, at room temperature any unsolubilised material was removed by centrifugation at $r_{AV} = 16,000 \text{ g}$ for 10 min. The supernatant was then layered onto a sucrose step gradient. The gradient consisted of 0.8, 0.6, 0.4, 0.2 M sucrose prepared in 20 mM Tris-HCl pH 8.0 containing 0.1%

(v/v) LDAO. The gradients were then centrifuged 16 h at $r_{AV}=149,000$ g at 4 °C. The upper-pigmented band contained the LH2 complexes and the lower pigmented band the LH1-RC complexes. The band containing LH2 complexes was collected and purified on a DE-52 cellulose column (Whatman). After a desalting step using a PD-10 column (GE Healthcare), the LH2 complexes were further purified by chromatography on a Resource-Q column (1 ml, GE Healthcare) and subsequently passed through a Superdex-200 column (1.6 cm i.d. × 100 cm, GE Healthcare). To ensure high purity, only fractions of the LH2 complex with a ratio between the absorption maximum at ~800 nm and the maximum at the protein absorption (A280) above 3.0 were collected for both spectroscopic analysis and crystallisation trials.

Prior to size-exclusion chromatography analysis, the HL and LL LH2s were detergent exchanged into DDM, accomplished by washing the LH2 sample five or six times with 20 mM Tris pH 8.0 containing 0.02% (w/v) DDM using a Vivaspinn2 centricon (50,000 MWCO, Sartoriusstedim Biotech). The DDM exchange was needed because one of the standards, RC-LH1 from *Rhodospirillum (Rsp.) rubrum* S1, is only stable in DDM. The intact size of the HL and LL LH2 complexes were determined by passing the purified LH2 complexes through a Superdex-200 gel filtration column (1.6 cm i.d. × 100 cm long, GE Healthcare) using 0.02% (w/v) DDM in 20 mM Tris-HCl pH 8.0 and comparing their elution profile with that of known standards also in 0.02% (w/v) DDM. The flow rate was 0.5 ml/min.

The purity and the size of the LH2 apoproteins were assessed by running on 12% NuPAGE Novex Bis-Tris mini gels (Invitrogen) using Novex Sharp protein standard (Invitrogen) molecular weight markers. The protein (10 µl, $OD_{850} = 40$ cm⁻¹) samples were mixed with 5 µl 300 mM dithiothreitol (DTT) and 5 µl NuPAGE LDS sample Buffer. After heating in a water bath at 70° C for 20 min, the mixtures were loaded onto the gel. NuPAGE SDS 1x running buffer (Invitrogen) in deionised water was used for the running buffer. The electrophoresis conditions were constant at 200 V for 40 min. The gels were stained with SimplyBlue SafeStain (Invitrogen) and destained with deionised water overnight.

The purified HL and LL LH2 complexes were sent to the FingerPrint Proteomic Facility, University of Dundee, for polypeptide identification. Each sample was first digested with trypsin in-gel prior to analysis by one-dimensional nano-liquid chromatography coupled to ESI-MS-MS using a 4000 QTRAP (Applied Biosystems) tandem MS system. The molecular mass of the LH2 peptide fragments were compared with hypothetical fragment masses predicted from their gene sequences, published online by UniProtKB/Swiss-Prot (based on the complete genomic sequence of *Rps. palustris* reported by Larimer *et al.* [18]).

Room temperature absorption spectra of cells, membranes and solubilised complexes were measured in a Shimadzu (UV-1700 Spectrophotometer) scanning from 250-950 nm. The 10K absorption spectra of LH2 complexes were measured using a Varian Cary E5 double-beam scanning spectrophotometer (Varian, Les Ulis, France). The LH2 samples were prepared for the low temperature spectra by the addition of 60% (v/v) glycerol in Tris buffer (20 mM, pH 8.0) containing 0.1% LDAO. The temperature of these samples was maintained by a Helium bath cryostat (Maico Metriks, Tartu, Estonia).

Circular dichroism (CD), fluorescence and fluorescence excitation spectroscopy were carried out according to Collins *et al.* [29]. The CD spectra were recorded with a Jasco J-815 spectropolarimeter (JASCO Inc., Easton, MD, USA) with a bandwidth to 4 nm. Samples were measured in a 1 mm, demountable quartz cuvette (Starna Scientific Limited, Hainault, Essex, England). Fluorescence emission and fluorescence excitation spectra were recorded using a Photon Technology International fluorometer (Birmingham, NJ, USA) equipped with a red-

sensitive avalanche photodiode detector (Advanced Photonics Inc., Camarillo, CA). Concentrated LH2 samples were prepared in 66 % (v/v) glycerol in 20 mM Tris-HCl buffer pH 8.0 containing 0.1 % LDAO. The low temperature environment was created using a liquid nitrogen cryostat (OptistatDN, Oxford Instruments, Bucks, UK).

The resonance Raman spectra were recorded with a Jobin-Yvon U1000 spectrometer equipped with a back-thinned CCD camera (Jobin Yvon Spectra ONE). The spectra were recorded with 90° geometry with the samples maintained at 77 K in a SMC-TBT flow cryostat (Air Liquide, Sassenage, France) cooled with liquid nitrogen. The samples were excited at 363.8 nm with a Coherent Inova 100 Ar+ laser with an incident intensity of less than 10 mW at the sample surface.

X-ray crystallography was used to attempt to determine the 3D-structures of both the HL and LL forms of LH2 from *Rps. palustris* 2.1.6. Initial crystallisation conditions for these proteins were obtained using commercial HT sparse matrix screens available from Molecular Dimension, Inc. using sitting-drop vapour diffusion. Robotic equipment, including the Cartesian Honeybee 8+1 nanodrop robot (Digilab (UK) Ltd.), the Microlab Star liquid dispensing robot (Hamilton Robotics, Inc) and the Rhombix Imager (ThermoFisher Scientific), was used in this process. The best conditions from the screens were then optimised in macroscale using a 24-well EasyXtall Tool tray (QIAGEN). These best conditions were as follows. The purified LH2 proteins were first washed three to four times with 20 mM Tris-HCl pH 8.0 buffer containing 0.1% (v/v) LDAO, then concentrated using a Vivaspin2 centricon (50,000 MWCO, Sartoriusstedim Biotech, UK). The final concentrations of LH2 proteins were adjusted to give an OD₈₅₀ of 80 cm⁻¹ for HL LH2 and OD₈₀₀ of 80 cm⁻¹ for LL LH2, respectively. 10 µl of the LH2 protein in 20 mM Tris-HCl pH 8.0 containing 0.1% (v/v) LDAO was pipetted onto a sitting drop bridge, while the reservoir chamber was filled with 1 ml of the solution containing 0.1 M Tris-HCl pH 9.5, 35% PEG 400, 0.1 M NaCl and 0.1 M MgCl₂ in case of HL LH2, and 0.1 M Tris-HCl pH 9.5, 37% PEG 400, 0.1 M NaCl and 0.1 M MgCl₂ in case of LL LH2. 10 µl of the reservoir solution was then mixed gently into the LH2 drop on the bridge. The crystallisation wells were subsequently sealed and the tray placed in a temperature controlled incubator (at 10 and/or 20 °C). The 10°C temperature was particularly important for the HL LH2 crystallisations as it reduced rapid precipitation. Crystals bigger than 300 µm in length grew within a few weeks. Useful LL LH2 crystals were also obtained from the following condition containing 50 mM glycine pH 10, 33% PEG 1000 and 50 mM NaCl in the reservoir. X-ray diffraction data from several of these crystals was collected at the European Synchrotron Radiation Facility in Grenoble, France, and at the Diamond Light Source, Oxfordshire, UK. All data sets were processed and scaled using the d*TREK program [30]. Further calculations were performed using the following programs; PHASER [31] for molecular replacement, MOLREP [32] for self rotation function, and REFMAC [33] for structure refinement, which are all parts of the CCP4 suite of programs [34]. Electron density maps were examined and Figure 10 was generated in program COOT [35].

Results

Growing the cells. Absorption spectra of whole cells grown at different light intensities were recorded and are presented in Figure 1. The high-light grown cells (Figure 1 black line) show an absorption spectrum in the NIR region, rather similar to those from *Rps. acidophila* and *Rba. sphaeroides*, with two strong absorption maxima at 805 nm and 862 nm that originate

from the HL LH2 complexes [8]. The B850 band is the most intense and has a shoulder at around 875 nm, indicating the presence of LH1-RC (core) complexes (Figure 1). As the light intensity is decreased, the NIR absorption spectra of the cells become markedly different. The 800 nm absorption band is more intense in the low-light grown cells, and ~850 nm band becomes correspondingly weaker and broader. As a result, the core 875 nm band is more apparent in the low-light (LL) grown cells (Figure 1 blue line). This situation reverses when the *Rps. palustris* cells are grown at the extreme lowest-light intensities, FLL1 and FLL2 (Figure 1 cyan and magenta lines), respectively. Under such extreme conditions, the intensity of the ~850 nm absorption band recovers towards its intensity seen in the high-light spectrum and narrows correspondingly. The relative molar ratio of LH2 to LH1 also varies depending on the light intensity at which the cells were grown. This ratio varies from approximately 3:1 at the highest light intensity used in the present study to 4.8:1 at the lowest light intensity used (Figure 2). This figure also shows how the ratio of the absorbance at 862 nm to that 805 nm varies with the light intensity at which the cells are grown. This ratio reflects the shift between the HL LH2 complex (high ratio) and the LL LH2 (low ratio). The value of this ratio reaches a minimum at 10 lx and then rises again at the lowest light intensities. This 'dip' in the '850/800' ratio as *Rps. palustris* cells are grown at progressively decreasing light intensities is consistently observed. The precise physiological reason for the return of a B800-850 'like' complex (often alongside the B800-820 complex) at very low light intensities has not yet been studied in any detail but a similar effect has also been previously reported for *Rps. acidophila* [8].

Purification and protein characterisation. The high- (HL) and low-light (LL) LH2 complexes were isolated and purified as described in the *Experimental* section. Their respective room temperature absorption spectra are presented in Figure 3A. The HL LH2 complexes have NIR Bchl *a* Q_y absorption bands at 803 and 857 nm (Figure 3A, solid line), whereas the LL LH2 complexes has absorption bands at 802 nm and 850 nm. The differences (Figure inset) in the intensities of the B800 and B850 absorption bands in the two types of purified LH2 complexes are consistent with those described above in the case of whole cells. If there were only two types of LH2 complexes possible i.e. HL LH2 and LL LH2 then overlaying the NIR absorption spectra of the LH2 fractions prepared from cells grown at the different light intensities should reveal an isosbestic point. If, however, there are more than two types of LH2 complex possible, then a single isosbestic point would not be expected with the overlaid absorption spectra. In order to make this measurement as clear as possible, the absorption spectra used for these comparisons were recorded at 10 K (Figure 4). These LH complexes are fully intact at cryogenic temperatures and their energy transfer reactions are essentially unchanged even down to 7 K [36]. At this temperature, the B800 absorption band sharpens and the B850 band both sharpens and red-shifts. The expanded potential isosbestic region at about 845 nm is shown in the inset in Figure 4. These overlaid spectra were very carefully normalised in the Q_x band region at ~595 nm and it can be seen that there is no single well-defined isosbestic point.

The polypeptide composition of the purified HL and LL LH2 complexes was investigated using NuPAGE Bis-Tris gel electrophoreses. Typical results are presented in Figure 5. Both the HL and LL LH2 complexes have four bands, two at ~10 kDa (H1 and L1) and two overlapping at ~7 kDa (H2 and L2). Due to the similarity between the different possible Puc polypeptides it is not possible from such gels to determine which of these bands correspond to which polypeptide. The identity of these polypeptides was, therefore, investigated using nLC-ESI-MS/MS. The bands seen on the gels were individually excised prior to mass spectroscopy analysis. The results of this analysis are shown in Table 1. In the case of HL LH2 complexes,

the two weak bands (H1) can be assigned as the PucA_a and PucA_b apoproteins and the two overlapping bands (H2) can be assigned as PucB_a and PucB_b apoproteins. In the case of LL LH2 complexes, the two weak bands (L1) bands can be assigned to the PucA_a and PucA_d apoproteins and the two overlapping L2 bands can be assigned as PucB_a, PucB_d and PucB_b apoproteins.

Size exclusion chromatography of the HL and LL LH2 complexes in the presence of DDM was used to estimate their relative size. Their elution profiles (Figure 6) were compared with the LH2 complex from *Rps. acidophila* 10050 (nonameric), the LH2 complex from *Phs. molischianum* (octameric) and RC-LH1 complex from *Rsp. rubrum* S1 (16-mer) [3, 3, 37]. Both the HL and LL LH2 complexes have similar sizes. Moreover, both these complexes appear to be slightly bigger than the LH2 from *Rps. acidophila*.

Spectroscopic characterisation. CD spectroscopy can be used to investigate the organisation of both Bchl *a* molecules and carotenoids in purple bacterial LH complexes [7, 38, 39]. The CD spectra of the HL and LL LH2 complexes in the NIR (700-950 nm) region are presented in Figure 7. There are common features shown in the spectra of both HL and LL LH2 complexes. There is a negative band at around B800 and an S-shaped band, with zero-crossing close to the absorption maximum of the B850 band. A detailed inspection of the CD spectrum of the HL LH2 complexes shows the presence of a negative band (-) at 794 nm and an S-shaped band (846 (+) and 873 (-) nm) with a zero-crossing at 857 nm. In the LL LH2 complexes the CD spectrum shows the negative B800 band is located at 789 nm. The magnitude of the S-shaped band at B850 decreases and its zero-crossing is red-shifted to 849 nm. There is an additional CD band (805 (+) and 819 (-) nm) in the spectrum of the LL LH2 complexes (Figure 7). Thus, the LL LH2 CD spectrum shows 789 (-) nm band and two S-shape bands (804(+)/819(-) nm and 839(+)/869(-) nm). The CD spectrum profiles in the UV-VIS (350-700 nm) region of the HL and LL LH2 complexes are very similar. There are positive bands in the Soret region (350-400 nm) and the Q_x region (589 nm) of Bchl *a* molecules, and a broad S-shaped profile in the carotenoid region (400-550 nm).

Figure 8 shows the fluorescence emission (dashed line) and excitation spectra (solid line) of the HL and LL LH2 complexes. Upon the excitation, λ_{ex} , at 800 nm, both HL and LL LH2 complexes show a single broad fluorescence emission band with the maximum intensity peaking at 897 and 892 nm, for HL and LL LH2 complexes, respectively. The excitation spectra (emission at 900 nm) of the HL and LL LH2 complexes exactly mirror their absorption spectra. This clearly shows that energy transfer reactions between the pigments within these isolated LH2 complexes are fully intact.

To elucidate further the interactions of the Bchl *a* molecules within these complexes Raman spectra were measured at 77 K in resonance conditions with the Soret electronic transition (363.8 nm). Under these conditions, all the Bchl *a* molecules of the LH2 complexes are expected to contribute more or less equally [40]. Figure 9 displays the high-frequency spectra (1590-1725 cm⁻¹) for the HL (black line), LL1 (red line), LL2 (green line) and LL (blue line) LH2 complexes. All the spectra are dominated by a band at 1609 cm⁻¹ attributed to the methane bridge stretching modes of Bchl *a* molecules having their central Mg²⁺ ion in its 5-coordination state [41]. The contributions from the carbonyl stretching modes (1620-1710 cm⁻¹) are relatively small in comparison and for this reason Figure 9B shows an enlarged view of most of this region (1640-1710 cm⁻¹). The bands centred at 1627, 1658, 1667 cm⁻¹ are attributed to the C3-acetyl and C13¹-keto Bchl *a* carbonyl stretching modes [42]. The band at 1697 cm⁻¹ is attributed to the free-from-interaction C13¹-keto carbonyl group of the B800 Bchl *a* [41]. It is evident that going from HL to LL *via* LL2 and LL1 there

is a progressive reduction of the ca 1620-1630 cm^{-1} region, which is accompanied by an increased intensity in the vibrational modes located between ca. 1650 and ca. 1680 cm^{-1} . From HL to LL there is also a small rearrangement in the spectral region of the keto carbonyl stretching mode of the B800 Bchl molecule (1697 cm^{-1}) but this is at the limit of detection (Figure 9B).

Crystallography. Reasonably sized (largest dimension > 300 μm) and quality HL and LL LH2 crystals were found to diffract X-rays at the synchrotron up to a resolution of about 4.5 Å and 4.7 Å, respectively. The absorption spectra of the redissolved crystals are shown in Figure 3B confirming that both HL and LL LH2 complexes were successfully crystallised. These crystals show monoclinic lattice symmetry, $P2_1$ or $C2$. Diffraction was, unfortunately, relatively anisotropic for all crystals tested, i.e. the diffraction limits were different in different spatial directions. Subsequently, a satisfactory merging of the diffraction data was only possible to a resolution of 6.3 Å in the case of the HL LH2 $P2_1$ crystal, 6.2 Å for the LL LH2 $P2_1$ crystal and 6.5 Å for the LL LH2 $C2$ crystal. This 'standard' data processing has excluded some of the highest resolution diffraction spots. Therefore, a special anisotropic scaling and ellipsoidal truncation with the use of the Diffraction Anisotropic Server [43] was applied to both data sets for the LL LH2 crystals in an attempt to correct for these effects. This 'anisotropic' processing produced a 5.0 Å dataset for the $C2$ crystal of LL LH2 and a 5.6 Å dataset for the $P2_1$ crystal. The summary of crystal data, including space groups, cell dimensions and data indexing and processing statistics for selected best HL and LL LH2 crystals is presented in Table 3. The unit cell volume and lattice symmetry together with the expected solvent contents of ca. 70% (crystals of *Rps. acidophila* 10050 LH2 [3, 4] have solvent contents of 69-73%, *Rps. acidophila* 7050 [5] 74%, and *Phs. molischianum* LH2 [6] 71%) revealed a presence of one whole ring of LH2 in the crystal asymmetric unit.

In order to extract the structural information from the intensity data (both 'standard' and 'anisotropic' processing data were used), self-rotation function (SRF) maps were calculated first for all the data sets to examine their internal symmetries [41]. These maps clearly show that the diffraction data were produced by the ring structure, with a unique direction of the ring axis in the crystal lattice. For all data sets the SRF maximum value for 9-fold symmetry, which coincides with the ring axis, is always slightly higher than the one for 8-fold symmetry. The difference, however, between them is within the one rms (root-mean-square) value of these SRF maps, therefore, the ring axis symmetry cannot be determined uniquely. Consistently, the belt of the ring 2-fold symmetries (perpendicular to the ring axis) is rather featurless, and does also not indicate the axial symmetry of the LH2 complex. For reference, the SRF map for our 1.85 Å LH2 structure from *Rps. acidophila* 10050 crystallised with the detergent LDAO (unpublished data) clearly shows nine pseudo 2-fold axes perpendicular to the ring axis and the SRF maximum value for the axial 9-fold symmetry is at 10.3 x map-rms level. Interestingly, the same data exhibits 8-fold and 10-fold symmetry components along the ring axis but at much lower levels, 4.3 and 5.6 x map-rms respectively, but still above the 3 x map-rms value. The SRF maximum values for the 8-fold and 9-fold symmetries for our low resolution *Rps. palustris* LH2 data are quite similar, and generally are not much higher than the values for the 7-fold or 10-fold, or even higher symmetries. The native Patterson maps were also calculated for these data sets but they were similarly not conclusive in distinguishing ring size. It is suggested, therefore, that there is rotational disorder in these LH2 complexes about their ring axes. This disorder could be due to rotation about the ring axis that is different than the basic angle between α/β -heterodimers (40° in case of *Rps. acidophila* LH2) for the LH2 complexes in different crystal lattice cells, or due to some degree of heterogeneity of the α/β -polypeptides.

Subsequently, a molecular replacement (MR) method was applied to investigate possible solutions for all the *Rps. palustris* LH2 data sets. The nonameric structure of the LH2 from *Rps. acidophila* 10050, the octameric one from *Phs. molischianum*, and the artificial/theoretical octameric model built from the *Rps. acidophila* 10050 α/β -heterodimer modules and their associated three BChls, were used as MR search models. Both *Rps. acidophila* based LH2 search models gave some satisfactory solutions in terms of the crystal lattice packing, whereas the *molischianum* LH2 solutions often produced clashes. Solutions using all three search models became possible, and often produced even better results, after some pruning of the N- and C-termini of α/β -polypeptides and/or removal of the protruding portions of the cofactors. However, the values of the associated figures of merit (the RFZ for rotational freedom, the TFZ for translational freedom and the LLG parameter, indicating the overall fit of the model in the crystal lattice [31]) showed that the solutions obtained with the *Rps. acidophila* 10050 nonameric LH2 model are clearly better than solutions obtained with an octameric *Phs. molischianum* LH2 model or with theoretical 'octameric *Rps. acidophila* LH2' model. Resulting figures of merit for all these cases are presented in Table 4 in the Supplementary Material. It is noticeable that the MR program [31] produces nine equivalent top solutions (with the highest similar LLG value) for the nonameric *Rps. acidophila* search model that all occupy the same space in the lattice with a rotation about the ring axis by 40° , suggestive of nine-fold symmetry in the LH2 complexes from *Rps. palustris*. If any lower LLG solutions were found, usually the next nine of them showed the ring rotated by 20° , effectively placing these solutions in-between the top ones. This confirms the observation found in the SRF maps that the LH2 ring position about the axis in our *Rps. palustris* LH2 crystals is not ordered. MR solutions obtained using the theoretical octameric '*Rps. acidophila* LH2 model' also occupy the same position in the crystal lattice as the nonameric *Rps. acidophila* model but the LLG values indicate that the agreement between the model and the experimental data is lower. This is most likely due to less satisfactory crystal packing as the diameter of the octamer is smaller than of the nonamer. In contrast, the *Phs. molischianum* search model gives many more top-LLG solutions (with the LLG values much lower than for the *Rps. acidophila* model) located in several different positions in the crystal lattice. These observations suggest that the overall shape of the *Rps. acidophila* LH2 complex, which is cylindrical and slightly conical, agrees better with the experimental data than the cylindrical but much less conical *Phs. molischianum* LH2 complex. The MR results also suggest that the nonameric ring architecture is preferred.

The best way to judge the quality of the MR solutions is through examination of the electron density maps. Map quality gives an indication of the quality of phasing of the diffraction data by the used search model and, therefore, about the topological similarity of the search model to the real structure from which the experimental data came. The electron density maps generated by Phaser [31] for the top MR solutions present a similar picture to the one described here. Figure 10 shows examples of such maps for the LL LH2 data in the $P2_1$ space group for the nonameric *Rps. acidophila* (views A and B) and octameric *Phs. molischianum* (views C and D) LH2 search models. Both models produced reasonable electron density for α -apoprotein helices but less complete ones for the β -apoprotein helices, although β -apoprotein helices calculated using the nonameric *Rps. acidophila* model were slightly more complete than those calculated using the other two models. Poor density for the β -apoprotein helices possibly results from a different topology of the *Rps. palustris* LH2 complex in comparison to the MR models. More important differences were observed for the Bchl macrocycles as the maps generated by the *Phs. molischianum* model do not reveal electron density that would correspond to the bacteriochlorin macrocycles of the tightly coupled B850 Bchl *a* molecules. In the corresponding region of the structure calculated from the *Rps.*

acidophila model there is a ring of electron density for these macrocycles. Moreover, the *Rps. acidophila* model also produces electron density for most of the bacteriochlorin macrocycles of the monomeric B800 Bchls, also not visible in the *Phs. molischianum* electron density. Electron density maps generated by the *Rps. acidophila* LH2 based theoretical octameric complex produced some unsatisfactory features similar to the *Phs. molischianum* LH2 model maps. The electron density obtained for the best solutions do not support the existence of an additional Bchl molecule. This has been suggested by Hartigan *et al.* [20] to be present below the B800 Bchl macrocycle in the LL LH2 structure from *Rps. palustris*. The lowest bands of electron density visible in Figure 10 are associated with the N-termini of the α -polypeptides and not with Bchl macrocycles.

Attempts were also made to refine some of the better solutions by the rigid-body refinement with the α -apoprotein helices, β -apoprotein helices and B800/B850 BChl molecules in separate rigid-body groups but the results were rather unsatisfactory. Instead, a different mode of refinement was used that relies upon 'jelly-body' and local NCS restraints implemented in the latest version of Refmac [33]. The values of R and R_{free} for various data are presented in the Table 4 in the Supplementary Material. These refinements have produced significant improvement of the R factors in comparison to rigid-body refinement. The best R factors, 0.358 for the HL LH2 $P2_1$ -data, and 0.382 for the LL LH2 $P2_1$ -data were obtained for the *Rps. acidophila* nonameric model, whereas the *Phs. molischianum* octameric model refined against the same data produced values of 0.513 and 0.479 respectively. The theoretical '*Rps. acidophila* octameric LH2 model' refined against the same data produced values of 0.575 and 0.494 respectively. The differences between these R factors again suggest the preference of the nonameric LH2 model for the *Rps. palustris* HL and LL LH2 data.

Maps from both the MR and the 'jelly-body' refinement at such low resolution are, however, heavily biased by whichever model is used. In order to test the model dependence on the phasing, omit maps were calculated for the *Rps. acidophila* and *Phs. molischianum* models by the removal of one α/β -polypeptide pair from each model. Figure 11 presents omit maps calculated for both HL (figures A and B) and LL (figures C and D) $P2_1$ -data. It is clear that density for the missing helices appears in maps for the *Rps. acidophila* nonameric model (in the 3-o'clock position). In contrast, the *Phs. molischianum* octameric model became slightly deformed and the maps reveal no density for the missing helices.

Discussion

The results of two previous studies on the polypeptide composition of the LH2 complexes from *Rps. palustris* 2.1.6 are compared with those obtained in this study (Table 2). Tadros *et al.* [16] proposed that there are two major polypeptides (PucAB_a and PucAB_b) and two minor polypeptides (PucAB_c and PucAB_d) present in the HL LH2 complex. It is not clear from their paper whether the two minor polypeptides were contaminants or not. Tharia *et al.* found that three peptide pairs (PucAB_a, PucAB_b and PucAB_d) were present in the HL LH2, while the LL LH2 only contained two pairs of polypeptides (PucAB_a and PucAB_d) [44]. Interestingly, the amount of β polypeptide present from the *pucAB_d* gene pair in the HL LH2 was much greater than that of the α polypeptide. No explanation was offered for this result. In the present study we have demonstrated that there are more than 2 types of LH2 complexes from *Rps. palustris* strain 2.1.6 synthesized under different light intensities. This is clear from the lack of an isosbestic point in Figure 4. It is not surprising, therefore, that our study shows that the LH2

complexes from *Rps. palustris* 2.1.6 are composed of a rather complicated mixture of α/β -polypeptides. In our hands two peptide pairs (PucAB_a and PucAB_b) were identified in the HL LH2 complex, while PucAB_a, PucAB_d and PucB_b-only were found in the LL LH2 complex (Table 1). The exact polypeptide composition varies depending on the precise growth conditions employed and with such closely related LH2 complexes it may well be almost impossible to separate them from each other.

As with the LH2 α -polypeptide from *Rps. acidophila* 10050, the pucA_a and pucA_b apoproteins from *Rps. palustris* strain 2.1.6 have tyrosine and tryptophan at positions 44 and 45 respectively. In the LH2 from *Rps. acidophila* 10050 the phenol sidechain of α -Tyr⁴⁴ and the indole sidechain of α -Trp⁴⁵ play important roles in formation of hydrogen bonds with the acetyl groups of the α -B850 Bchl and the β -B850 Bchl respectively. These residues are replaced by phenylalanine and methionine in the pucA_d apoprotein of LL LH2 from *Rps. palustris* 2.1.6. In the B800-820 LH2 from *Rps. acidophila* 7050 the replacement of Tyr⁴⁴ and Trp⁴⁵ with Phe⁴⁴ and Leu⁴⁵, respectively, results in a loss of H-bond donors for the H-bonds to the Bchl acetyl groups as found in B800-850 LH2 from *Rps. acidophila* 10050 [5]. However, in the B800-820 LH2 the acetyl group of the α -B850 Bchl forms a new hydrogen bond instead, to a hydroxyl of α -Tyr⁴¹, which was a phenylalanine in B800-850 LH2. The acetyl group of the β -B850 Bchl is not hydrogen bonded in the crystal structure of B800-820 LH2. In the B800-820 LH2 complex the Bchl C3-acetyl groups are rotated out-of-plane with respect to the bacteriochlorin plane [3, 5]. This effect reduces the extent of π -conjugation in the Bchl and results in a blue shift of its site energy [45, 46], reflected in the shift of the absorption band from 850 nm to 820 nm.

In each α/β -polypeptide, three Bchl molecules contribute to the six vibrational modes present in the high frequency region (1620-1720 cm⁻¹) of a Raman spectrum. These modes correspond to the C3-acetyl and C13¹-keto Bchl *a* carbonyl stretching modes [47] and were distinguishable from one another in the following systematic study using the B800-850 LH2 complex from *Rba. sphaeroides*. The replacement of α -Tyr⁴⁴ and α -Tyr⁴⁵, to Phe-Tyr (single mutant) or to Phe-Leu (double mutant) produced B800-839 and B800-826 complexes respectively [48]. Resonance Raman studies of these mutants identified the breakage of one or two H-bonds, respectively, between the protein residues and the respective C3-acetyl carbonyl groups of the B850 Bchls [48]. The removal of an H-bond to the acetyl carbonyl group was signalled by a shift of the Raman peak from the wild-type LH2 at 1635 cm⁻¹ to a position expected for a non H-bonded, free acetyl carbonyl, i.e. 1659 cm⁻¹. It was further demonstrated, using wild-type and mutant antenna complexes, that there is a consistent linear relationship between the downshift in the Bchl *a* C3 acetyl stretching mode and the red-shift in the Q_y absorption maximum [49]. This is because, in these complexes, the α/β -polypeptide dimers were considered to contain only one type of α -polypeptide and one type of β -polypeptide (the existence of the second β -polypeptide in the LH2 complex from *Rba. sphaeroides* [50] was not known at this time but its homology to the *puc1B*-encoded-polypeptide is such that it does contribute to any spectral contamination).

In a homogenous LH sample all the Bchl *a* molecules are expected to contribute more or less equally to the Raman signal when probed in the Soret transition, but under pre-resonant conditions with the Q_y absorption band the relative signal from the red-most chromophore will be enhanced [40, 51]. Thus, when compared to Soret excitation the positions of the vibrational bands will be the same, albeit with different intensities. However, if a mixed population of LH complexes is present the observed intensities and positions of the carbonyl vibrational modes will not necessarily be the same due to the presence of sub-populations

having different Bchl *a* Q_y-transitions. This is exactly what happens in *Rps. palustris* when LL LH2 is compared to its HL variant [25]. This previous work proposed that LL LH2 contains rings containing multiple α -polypeptides since no native-like B800-820 LH2 (also called LH3) was observed [25]. However, this previous study did not analyse the polypeptide composition, rather relied solely on the comparison of the electronic absorption properties together with other studies where the polypeptide composition had been established [25]. In this present study, where the absorption (Figure 3) and Raman spectra (Figure 9) mirror the previous Raman study, and where the polypeptide composition has been established, it can now be unambiguously concluded that rings with mixtures of α -polypeptides (PucA_a and PucA_d, see Table 1) are indeed present in LL LH2 complexes from *Rps. palustris*. The PucA_d protein is not able to form H-bonds with Bchl *a* molecules to produce a B800-850 LH2. Furthermore, going from HL to LL, *via* LL2 and LL1, there is a progressive reduction in the apparent strength of the Bchl *a* H-bond network (Figure 9), which when combined with the evolution of the blue-shift in the B850 Bchl *a* Q_y-transition (Figure 3), suggests that the population with mixed 'rings' containing PucA_d increases as the growth conditions are pushed further towards lower light intensities.

The low resolution X-ray diffraction obtained for the HL and LL LH2 crystals from *Rps. palustris* 2.1.6 is a result of the limited crystalline order and that feature of these crystals could be, in part, due to the LH2 ring heterogeneity. Such heterogeneity could also contribute to the rotational disorder about the LH2-ring axis apparent in the self-rotation functions. The MR solutions obtained with the X-ray diffraction data suggest that the most probable structure for both the HL and LL LH2 from *Rps. palustris* 2.1.6 is a nonamer and that the overall shape of the complex is more similar to the *Rps. acidophila* LH2 than to the *Phs. molischianum* LH2. Molecular sieve chromatography also suggests that both these HL and LL LH2 complexes from *Rps. palustris* 2.1.6 are nonameric. Higher resolution diffracting crystals, if they can be produced, are now required in order to try and obtain a better picture of the exact details of the LH2 ring heterogeneity. However, since there are more than two types of LH2 complexes present and since it is not clear that any of these complexes can be individually purified, this may well prove to be a very difficult challenge. A possible way out of this impasse may be through the recent advances in mass spectrometry that now allow large, detergent solubilised multi-protein complexes to 'fly' as intact complexes. Experiments are now underway trying to develop the use of this technique with the various LH2 complexes from *Rps. palustris* (and indeed on many other interesting photosynthetic LH complexes in our laboratory) and it is hoped that these results will prove rewarding in the future.

Acknowledgements

We gratefully acknowledge Dr. James Sturgis for providing us with the LH2 complexes from *Phs. molischianum*. We acknowledge the European Synchrotron Radiation Facility for provision of synchrotron radiation facilities and we would like to thank Dr. S. McSweeney, Dr. G.A. Leonard, Dr. L. Terradot, Dr. H. Belrhali, and Dr. S. Brockhauser, for their assistance in using beamlines ID29 (twice), ID14-4, BM14 and ID23-2. We also acknowledge the support of the Diamond Light Source for provision of beamtime at station I04.

Funding

This work was supported as part of the Photosynthetic Antenna Research Center (PARC), an Energy Frontier Research Center funded by the U.S. Department of Energy, Office of Science, Office of Basic Energy Sciences under Award Number DE-SC 0001035. AWR, ATG and RJC acknowledge financial support from the EPSRC.

References

- 1 Blankenship, R. E. (2002) Molecular mechanisms of photosynthesis. Blackwell Science, Oxford
- 2 Roszak, A. W., Howard, T. D., Southall, J., Gardiner, A. T., Law, C. J., Isaacs, N. W. and Cogdell, R. J. (2003) Crystal structure of the RC-LH1 core complex from *Rhodospseudomonas palustris*. *Science*. **302**, 1969-1972
- 3 McDermott, G., Prince, S. M., Freer, A. A., Hawthornthwaite-lawless, A. M., Papiz, M. Z., Cogdell, R. J. and Isaacs, N. W. (1995) Crystal structure of an integral membrane light-harvesting complex from photosynthetic bacteria. *Nature*. **374**, 517-521
- 4 Papiz, M. Z., Prince, S. M., Howard, T., Cogdell, R. J. and Isaacs, N. W. (2003) The structure and thermal motion of the B800-850 LH2 complex from *Rps. acidophila* at 2.0 Å resolution and 100K: new structural features and functionally relevant motions. *J Mol Biol*. **326**, 1523-1538
- 5 McLuskey, K., Prince, S. M., Cogdell, R. J. and Isaacs, N. W. (2001) The crystallographic structure of the B800-820 LH3 light-harvesting complex from the purple bacteria *Rhodospseudomonas acidophila* strain 7050. *Biochemistry*. **40**, 8783-8789
- 6 Koepke, J., Hu, X., Muenke, C., Schulten, K. and Michel, H. (1996) The crystal structure of the light-harvesting complex II (B800-850) from *Rhodospirillum molischianum*. *Structure*. **4**, 581-597
- 7 Cogdell, R. J. and Scheer, H. (1985) Circular-dichroism of light-harvesting complexes from purple photosynthetic bacteria. *Photochem Photobiol*. **42**, 669-678
- 8 Gardiner, A. T., Cogdell, R. J. and Takaichi, S. (1993) The effect of growth conditions on the light-harvesting apparatus in *Rhodospseudomonas acidophila*. *Photosynth Res*. **38**, 159-167
- 9 Bissig, I., Brunisholz, R. A., Suter, F., Cogdell, R. J. and Zuber, H. (1988) The complete amino acid sequences of the B800-850 antenna polypeptides from *Rhodospseudomonas acidophila* strain 7750. *Z Naturforsch [C]*. **43**, 77-83
- 10 Gardiner, A. T., Mackenzie, R.C., Barrett, S.J., Kaiser, K. and Cogdell, R. J. (1996) the purple photosynthetic bacterium *Rhodospseudomonas acidophila* contains multiple puc peripheral antenna complex (LH2) genes: Cloning and initial characterisation of four β/α pairs. *Photosynth. Res*. **49**: 223-235
- 11 Hayashi, H., Miyao, M. and Morita, S. (1982) Absorption and fluorescence spectra of light-harvesting bacteriochlorophyll-protein complexes from *Rhodospseudomonas palustris* in the near-infrared region. *J Biochem*. **91**, 1017-1027
- 12 Evans, M. B., Hawthornthwaite, A. M. and Cogdell, R. J. (1990) Isolation and characterization of the different B800-850 light-harvesting complexes from low-light and high-light grown cells of *Rhodospseudomonas palustris*, strain 2.1.6. *Biochim Biophys Acta*. **1016**, 71-76
- 13 van Mourik, F., Hawthornthwaite, A. M., Vonk, C., Evans, M. B., Cogdell, R. J., Sundström, V. and Vangrondele, R. (1992) Spectroscopic characterization of the low-light B800-850 light-harvesting complex of *Rhodospseudomonas palustris* strain 216. *Biochim Biophys Acta*. **1140**, 85-93

- 14 Hayashi, H., Nozawa, T., Hatano, M. and Morita, S. (1982) Circular dichroism of bacteriochlorophyll a in light-harvesting bacteriochlorophyll-protein complexes from *Rhodospseudomonas palustris*. *J Biochem.* **91**, 1029-1038
- 15 Hayashi, H., Nakano, M. and Morita, S. (1982) Comparative studies of protein properties and bacteriochlorophyll contents of bacteriochlorophyll-protein complexes from spectrally different types of *Rhodospseudomonas palustris*. *J Biochem.* **92**, 1805-1811
- 16 Tadros, M. H. and Waterkamp, K. (1989) Multiple copies of the coding regions for the light-harvesting B800-850 alpha- and beta-polypeptides are present in the *Rhodospseudomonas palustris* genome. *EMBO J.* **8**, 1303-1308
- 17 Tadros, M. H., Katsiou, E., Hoon, M. A., Yurkova, N. and Ramji, D. P. (1993) Cloning of a new antenna gene cluster and expression analysis of the antenna gene family of *Rhodospseudomonas palustris*. *Eur J Biochem.* **217**, 867-875
- 18 Larimer, F. W., Chain, P., Hauser, L., Lamerdin, J., Malfatti, S., Do, L., Land, M. L., Pelletier, D. A., Beatty, J. T., Lang, A. S., Tabita, F. R., Gibson, J. L., Hanson, T. E., Bobst, C., Torres, J. L., Peres, C., Harrison, F. H., Gibson, J. and Harwood, C. S. (2004) Complete genome sequence of the metabolically versatile photosynthetic bacterium *Rhodospseudomonas palustris*. *Nat Biotechnol.* **22**, 55-61
- 19 Law, C. J. and Cogdell, R. (2008) The light-harvesting system of purple anoxygenic photosynthetic bacteria. In *Primary Processes of Photosynthesis, Part 1 Principle and Apparatus* (Renger, G., ed.). pp. 205-259, RSC Publishing, Cambridge
- 20 Hartigan, N., Tharia, H. A., Sweeney, F., Lawless, A. M. and Papiz, M. Z. (2002) The 7.5-Å electron density and spectroscopic properties of a novel low-light B800 LH2 from *Rhodospseudomonas palustris*. *Biophys J.* **82**, 963-977
- 21 Evans, K., Fordham-Skelton, A. P., Mistry, H., Reynolds, C. D., Lawless, A. M. and Papiz, M. Z. (2005) A bacteriophytochrome regulates the synthesis of LH4 complexes in *Rhodospseudomonas palustris*. *Photosynth Res.* **85**, 169-180
- 22 Scheuring, S., Goncalves, R. P., Prima, V. and Sturgis, J. N. (2006) The photosynthetic apparatus of *Rhodospseudomonas palustris*: Structures and organization. *J. Mol. Biol.* **358**, 83-96
- 23 Mascle-Allemand, C., Duquesne, K., Lebrun, R., Scheuring, S. and Sturgis, J. N. (2010) Antenna mixing in photosynthetic membranes from *Phaeospirillum molischianum*. *Proc Natl Acad Sci U S A.* **107**, 5357-5362
- 24 Hess, S., Feldchtein, F., Babin, A., Nurgaleev, I., Pullerits, T., Sergeev, A. and Sundström, V. (1993) Femtosecond energy-transfer within the LH2 peripheral antenna of the photosynthetic purple bacteria *Rhodobacter sphaeroides* and *Rhodospseudomonas palustris* LL. *Chem Phys Lett.* **216**, 247-257
- 25 Gall, A. and Robert, B. (1999) Characterization of the different peripheral light-harvesting complexes from high- and low-light grown cells from *Rhodospseudomonas palustris*. *Biochemistry.* **38**, 5185-5190
- 26 Brotosudarmo, T. H., Kunz, R., Böhm, P., Gardiner, A. T., Moulisova, V., Cogdell, R. J. and Köhler, J. (2009) Single-molecule spectroscopy reveals that individual low-light LH2 complexes from *Rhodospseudomonas palustris* 2.1.6. have a heterogeneous polypeptide composition. *Biophys J.* **97**, 1491-1500
- 27 Moulisova, V., Luer, L., Hoseinkhani, S., Brotosudarmo, T. H., Collins, A. M., Lanzani, G., Blankenship, R. E. and Cogdell, R. J. (2009) Low light adaptation: energy transfer processes in different types of light harvesting complexes from *Rhodospseudomonas palustris*. *Biophys J.* **97**, 3019-3028
- 28 Böse, S. K. (1963) *Bacterial photosynthesis*. Antioch Press, Yellow Springs, Ohio

- 29 Collins, A. M., Xin, Y. Y. and Blankenship, R. E. (2009) Pigment organization in the photosynthetic apparatus of *Roseiflexus castenholzii*. *Biochim Biophys Acta-Bioenergetics*. **1787**, 1050-1056
- 30 Pflugrath, J. (1999) The finer things in X-ray diffraction data collection. *Acta Crystallogr. Sect D Biol. Crystallogr.* **55**, 1718-1725
- 31 McCoy, A. J., Grosse-Kunstleve, R. W., Adams, P. D., Winn, M. D., Storoni, L. C. and Read, R. J. (2007) Phaser crystallographic software. *J. Appl. Crystallogr.* **40**, 658-674
- 32 Vagin, A. and Teplyakov, A. (1997) MOLREP: an automated program for molecular replacement. *J Appl Crystallogr.* **30**, 1022-1025
- 33 Murshudov, G. N., Skubak, P., Lebedev, A.A., Pannu, N.S., Steiner, R.A., Nicholls, R.A., Winn, M.D., Long, F. and Vagin, A.A. (2011) REFMAC 5 for the refinement of macromolecular crystal structures. *Acta Crystallogr. Sect D Biol. Crystallogr.* **67**, 355-367
- 34 CCP4. (1994) The CCP4 suite: programs for protein crystallography. *Acta Crystallogr. Sect D Biol. Crystallogr* **50**, 760-763
- 35 Emsley, P., Lohkamp, B., Scott, W. G. and Cowtan, K. (2010) Features and development of Coot. *Acta Crystallogr. Sect D Biol. Crystallogr* **66**, 486-501
- 36 Zazubovich, V., Jankowiak, R. and Small, G.J. (2002) On B800 → B800 energy transfer in the LH2 complex of purple bacteria. *J Luminescence* **98**, 123-129
- 37 Karrasch, S., Bullough, P. A. and Ghosh, R. (1995) The 8.5-angstrom projection map of the light-harvesting complex-I from *Rhodospirillum rubrum* reveals a ring composed of 16 subunits. *EMBO Journal*. **14**, 631-638
- 38 Koolhaas, M. H. C., van der Zwan, G., Frese, R. N. and van Grondelle, R. (1997) Red shift of the zero crossing in the CD spectra of the LH2 antenna complex of *Rhodopseudomonas acidophila*: A structure-based study. *J Phys Chem B*. **101**, 7262-7270
- 39 Georgakopoulou, S., Frese, R. N., Johnson, E., Koolhaas, C., Cogdell, R. J., van Grondelle, R. and van der Zwan, G. (2002) Absorption and CD spectroscopy and modeling of various LH2 complexes from purple bacteria. *Biophys J*. **82**, 2184-2197
- 40 Gall, A., Fowler, G. J., Hunter, C. N. and Robert, B. (1997) Influence of the protein binding site on the absorption properties of the monomeric bacteriochlorophyll in *Rhodobacter sphaeroides* LH2 complex. *Biochemistry*. **36**, 16282-16287
- 41 Robert, B. and Lutz, M. (1985) Structures of Antenna Complexes of Several Rhodospirillales from Their Resonance Raman-Spectra. *Biochim Biophys Acta*. **807**, 10-23
- 42 Fowler, G. J. S., Sockalingum, G. D., Robert, B. and Hunter, C. N. (1994) Blue Shifts in Bacteriochlorophyll Absorbency Correlate with Changed Hydrogen-Bonding Patterns in Light-Harvesting 2 Mutants of *Rhodobacter sphaeroides* with Alterations at Alpha-Tyr-44 and Alpha-Tyr-45. *Biochem J*. **299**, 695-700
- 43 Strong, M., Sawaya, M. R., Wang, S., Phillips, M., Cascio, D. and Eisenberg, D. (2006) Toward the structural genomics of complexes: crystal structure of a PE/PPE protein complex from *Mycobacterium tuberculosis*. *Proc Natl Acad Sci U S A*. **103**, 8060-8065
- 44 Tharia, H. A., Nightingale, T. D., Papiz, M. Z. and Lawless, A. M. (1999) Characterisation of hydrophobic peptides by RP-HPLC from different spectral forms of LH2 isolated from *Rps. palustris*. *Photosynth Res*. **61**, 157-167
- 45 Hanson, L. K. (1991) Molecular orbital theory of monomer pigments. In *Chlorophylls* (Scheer, H., ed.). pp. 993-1014, CRC Press, Boca Raton
- 46 Gudowskanowak, E., Newton, M. D. and Fajer, J. (1990) Conformational and environmental effects on bacteriochlorophyll optical spectra: correlations of calculated spectra with structural results *J. Phys. Chem.* **94**, 5795-5801
- 47 Sturgis, J. N., Jirsakova, V., Reiss-Husson, F., Cogdell, R. J. and Robert, B. (1995) Structure and properties of the bacteriochlorophyll binding site in peripheral light-harvesting complexes of purple bacteria. *Biochemistry*. **34**, 517-523

- 48 Fowler, G. J. S., Visschers, R. W., Grief, G. G., Vangrondelle, R. and Hunter, C. N. (1992) Genetically modified photosynthetic antenna complexes with blueshifted absorbency bands. *Nature*. **355**, 848-850
- 49 Sturgis, J. N. and Robert, B. (1997) Pigment binding-site and electronic properties in light-harvesting proteins of purple bacteria. *J Phys Chem B*. **101**, 7227-7231
- 50 Zeng, X., Choudhary, M. and Kaplan, S. (2003) A second and unusual *pucBA* operon of *Rhodobacter sphaeroides* 2.4.1: genetics and function of the encoded polypeptides. *J Bacteriol*. **185**, 6171-6184
- 51 Sturgis, J. N., Gall, A., Ellervee, A., Freiberg, A. and Robert, B. (1998) The effect of pressure on the bacteriochlorophyll a binding sites of the core antenna complex from *Rhodospirillum rubrum*. *Biochemistry*. **37**, 14875-14880
- 52 Fowler, G. J. and Hunter, C. N. (1996) The synthesis and assembly of functional high and low light LH2 antenna complexes from *Rhodopseudomonas palustris* in *Rhodobacter sphaeroides*. *J Biol Chem*. **271**, 13356-13361

Table 1. Peptide identification of the gel bands (H1, H2, L1 and L2) from the HL and LL LH2 complexes by nLC-ESI-MS/MS. The residues of the α -polypeptides at position 44 and 45 are highlighted in yellow.

LH2	Peptide residues (The detected fraction is underlined)	Predicted mass of the fragment	Observed mass of the fragment	Assignment
HL				
Band H1	-----10-----20-----30-----40-----50-----60----- MNQARIWTVV KPTVGLPLLL GSVTVIAILV HFAVLSHTTW FSK <u>YW</u> NGKAA AIESSVNVG- ----- 59	1016.5	1016.5	PucA _a
	MNQGRITVV NPGVGLPLLL GSVTVIAILV HYAVLSNTTW FPK <u>YW</u> NGATV AAPAAAPAPA APAAKK 66	2036.1	2036.1	PucA _b
Band H2	MADKTLTGLT <u>VEESEELHKH</u> VIDGTRIFGA IAIVAHFLAY VYSPWLH--- - 47	1684.9	1684.9	PucB _a
	MADDPNKVWP TGLTIAESEE <u>LHKHVIDGTR</u> IFGAIIVAH FLAYVYSPWL H 51	1808.9	1808.9	PucB _b
LL				
Band L1	-----10-----20-----30-----40-----50-----60----- MNQARIWTVV KPTVGLPLLL GSVTVIAILV HFAVLSHTTW FSK <u>YW</u> NGKAA AIESSVNVG- ----- 59	1016.5	1016.5	PucA _a
	MNQGRITVV KPTVGLPLLL GSVAIMVFLV HFAVLTHTTW VAK <u>FM</u> NGKAA AIESSIKAV- ----- 59	889.5	889.5	PucA _d
Band L2	MADKTLTGLT <u>VEESEELHKH</u> VIDGTRIFGA IAIVAHFLAY VYSPWLH--- - 47	1684.9	1684.9	PucB _a
	MVDDPNKVWP TGLTIAESEE <u>LHKHVIDGSR</u> IFVAIAIVAH FLAYVYSPWL H 51	1808.9	1808.9	PucB _d
	MADDPNKVWP TGLTIAESEE <u>LHKHVIDGTR</u> IFGAIIVAH FLAYVYSPWL H 51	3165.7	3165.7	PucB _b

Table 2. Polypeptide composition of LH2 complexes found in *Rps. palustris* 2.1.6.

	High-light LH2	Low-light LH2
Tadros <i>et al.</i> (1989)[16]	PucAB _a , PucAB _b , PucAB _c and PucAB _d	-
Tharia <i>et al.</i> (1999)[44]	PucAB _a , PucAB _b and PucAB _d	PucAB _a and PucAB _d
This work	PucAB _a and PucAB _b	PucAB _a , PucAB _d and PucB _b

THIS IS NOT THE VERSION OF RECORD - see doi:10.1042/BJ20110575

Table 3. X-ray diffraction processing statistics for the LH2 crystals from *Rps. palustris* 2.1.6; the values in parentheses refer to the highest-resolution shell of data.

LH2 complex	HL LH2	LL LH2	
Space group	$P2_1$	$C2$	$P2_1$
Unit cell dimensions			
$a/ b/ c$ (Å)	94.62/124.28/95.07	157.78/114.00/146.79	98.37/129.67/98.37
$\alpha/ \beta/ \gamma$ (°)	90.00/111.20/90.00	90.00/114.58/90.00	90.0/110.12/90.00
Resolution range (Å)	39.13-6.30 (6.52-6.30)	44.71-6.50 (6.73-6.50)	42.53-6.20 (6.42-6.20)
Total no. of measured data	24299	23297	31357
No. of unique reflections	4457	4690	5257
Average redundancy	5.45 (5.76)	4.97 (5.33)	5.96 (6.22)
Completeness (%)	99.2 (100.0)	98.6 (100.0)	98.5 (99.8)
$R_{\text{merge}} = \frac{\sum_{hkl} \sum_i I_i(hkl) - \langle I(hkl) \rangle }{\sum_{hkl} \sum_i I_i(hkl)}$	0.057 (0.400)	0.046 (0.479)	0.057 (0.558)
Mean signal to noise ratio, $\langle I/\sigma \rangle$	14.4 (1.7)	15.1 (1.9)	11.1 (2.0)

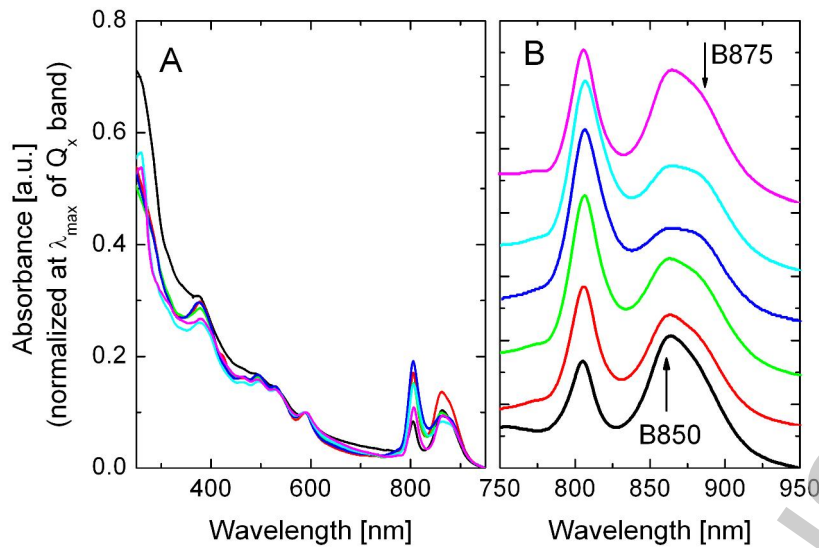


Figure 1. (A) Room temperature absorption spectra of whole cells from *Rps. palustris* 2.1.6 grown at different light intensities: high-light (HL, black line), intermediate 1 low-light (LL1, red line), intermediate 2 low-light (LL2, green line), low-light (LL, blue line), far 1 low-light (FLL1, cyan line) and far 2 low-light (FLL2, magenta line). (B) A magnification of the near infrared region (NIR) region is shown.

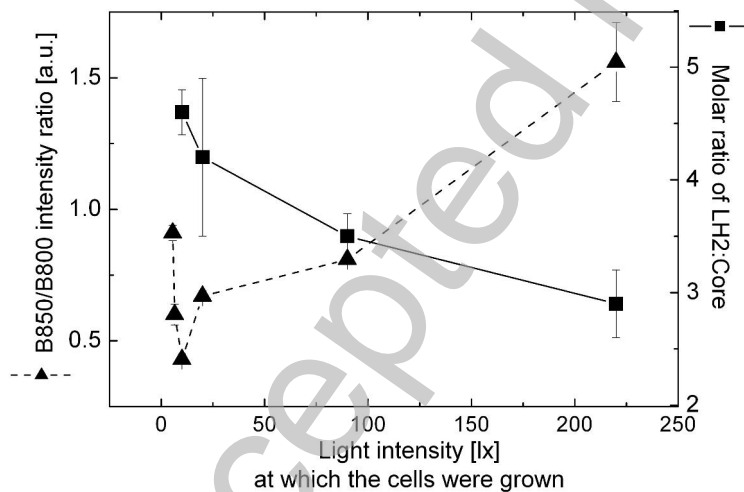


Figure 2. The intensity ratio of the bands B850:B800 of the whole cell RT absorption spectra (dashed line) and molar ratio of LH2:Core (solid line) depending on the light intensity at which the cells were grown. The bars indicate standard deviation with $n = 4$.

THIS IS NOT THE VERSION OF RECORD - see doi:10.1042/BJ20110575

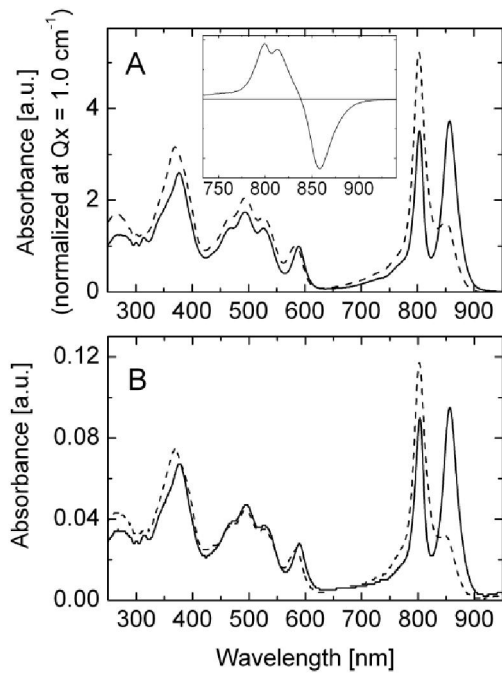


Figure 3. Room temperature absorption spectra of HL (solid line) and LL (dashed line) LH2 complexes from *Rps. palustris* 2.1.6. (A) in solution and from (B) dissolved crystals. Inset is the difference spectra HL-LL LH2 in the near infrared region (NIR) region.

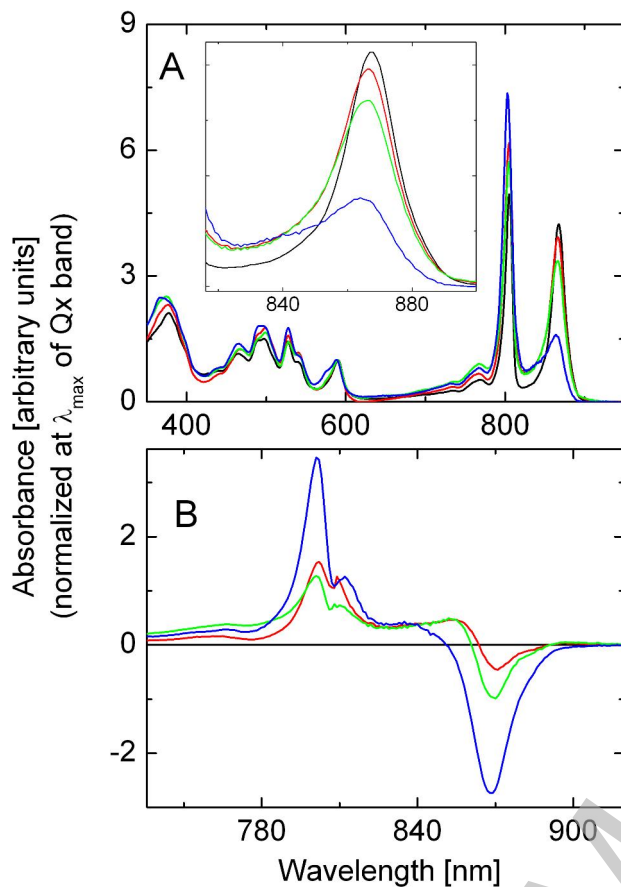


Figure 4. Absorption spectra at 10 K of HL (black line), LL1 (red line), LL2 (green line) and LL (blue line) LH2 complexes. (A) The absorption spectra in the 350-950 nm region. The inset is a magnification of the near infrared region (NIR) region. (B) Difference spectra of LL1-HL (red line), LL2-HL (green line) and LL-HL (blue line) recorded in the NIR region. The spectra are normalised at Q_x band.

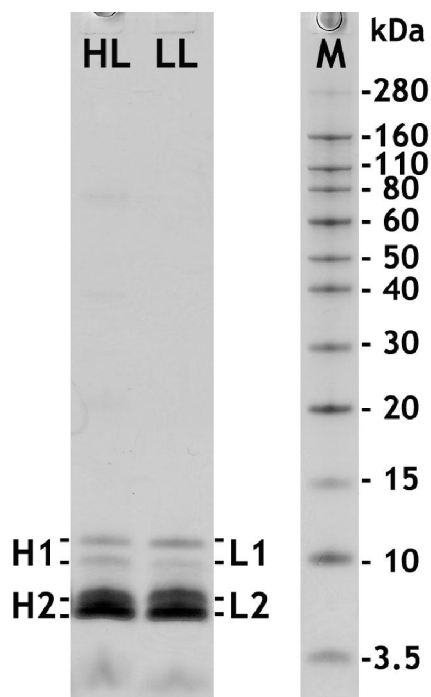


Figure 5. A denaturing SDS / 10% Bis-Tris gel profile of the apoproteins from the HL and LL LH2 complexes after their purification. The apoprotein bands are indicated as L1, L2, H1 and H2. The band at the bottom (~3.5 kDa) corresponds to pigments and lipids and can be removed by prior delipidation of the complexes (data not shown).

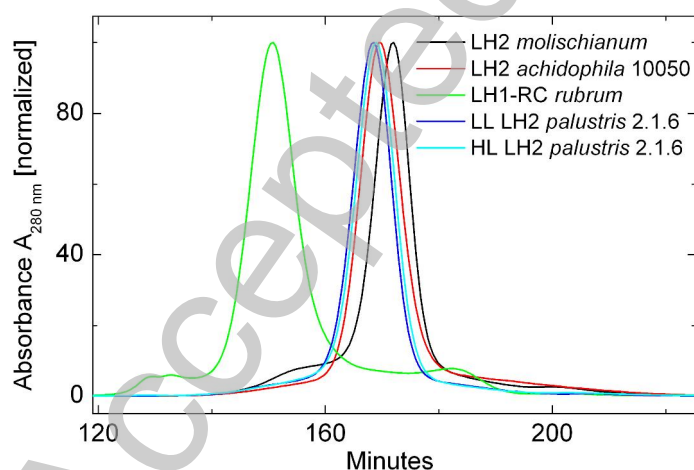


Figure 6. Size exclusion (Superdex S-200) elution profile of HL and LL LH2 from *Rps. palustris* 2.1.6 compared with LH2 from *Rps. acidophila* 10050 (nonameric), LH2 complex from *Phs. molischianum* (octameric) and RC-LH1 complex from *Rsp. rubrum* S1 (16-mer).

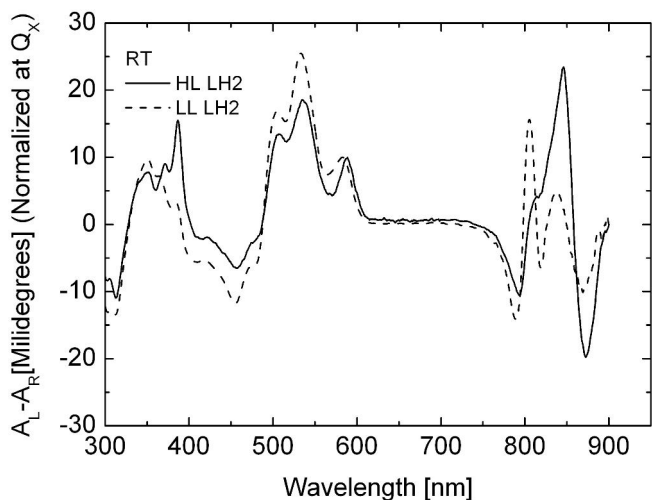


Figure 7. Room temperature circular dichroism (CD) spectra of HL (solid line) and LL LH2 (dashed line) from *Rps. palustris* 2.1.6. The spectra were normalised in the Q_x band.

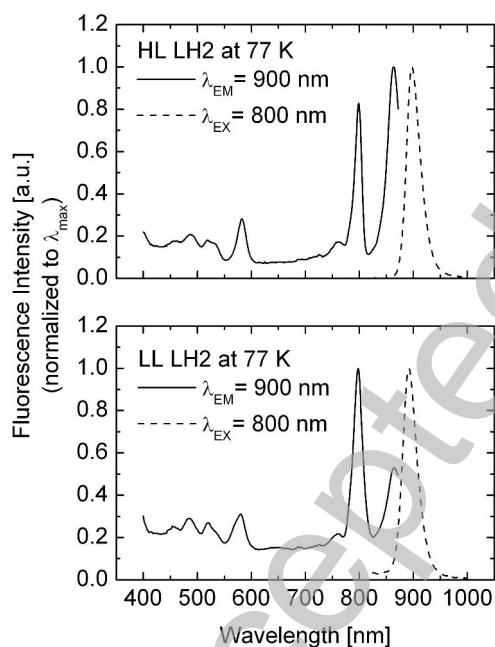


Figure 8. Fluorescence excitation (solid line) and emission (dashed line) spectra of HL and LL LH2 from *Rps. palustris* 2.1.6 recorded at 77 K. The fluorescence emission spectra were obtained by excitation at 800 nm, while the fluorescence excitation spectra were recorded monitoring the emission at 900 nm. The spectra are normalized at the λ_{max} .

THIS IS NOT THE VERSION OF RECORD - see doi:10.1042/BJ20110575

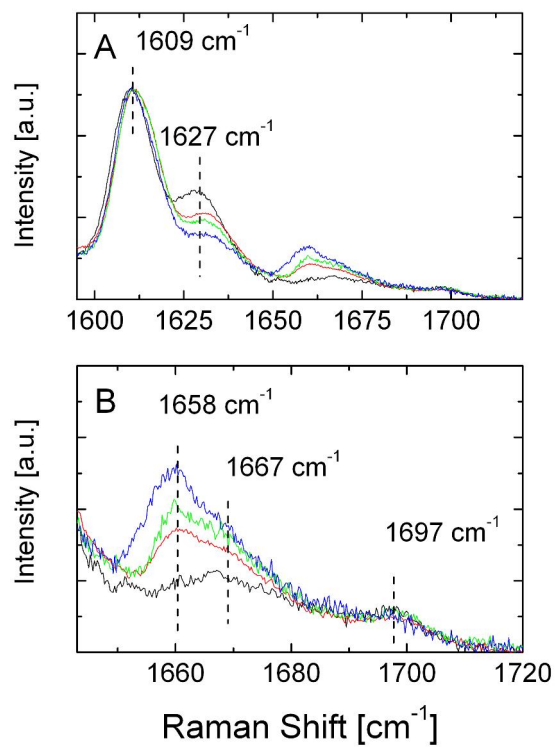


Figure 9. (A) 77 K UV resonance Raman spectra of the HL (black line), LL1 (red line), LL2 (green line) and LL (blue line) LH2 from *Rps. palustris* 2.1.6. (B) The magnification at carbonyl region (1640-1710 cm⁻¹). The spectra were normalised at the 1609 cm⁻¹ peak. The excitation wavelength was 363.8 nm.

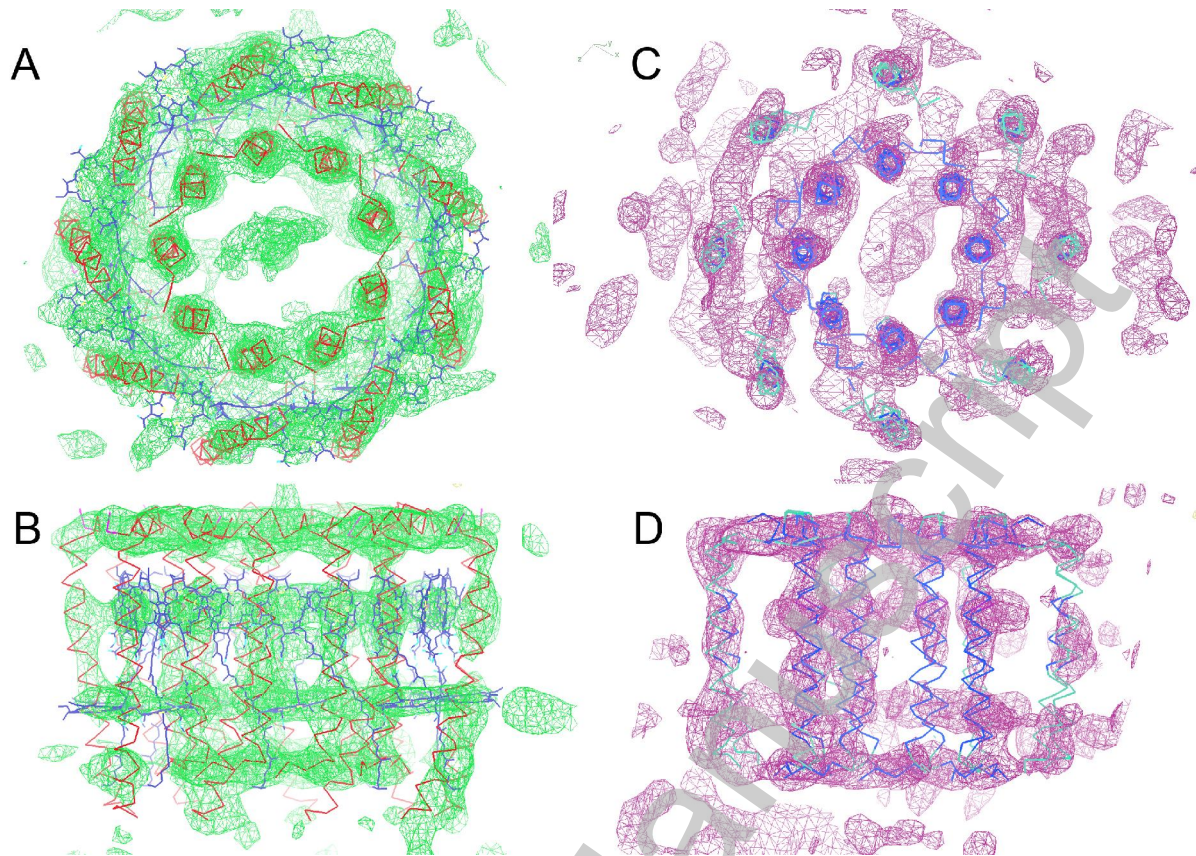


Figure 10. Low resolution (5.6 Å) electron density map (at 1.5 σ level) for the *Rps. palustris* LL LH2 $P2_1$ -diffraction data generated by molecular replacement (MR) using the B800-850 LH2 from *Rps. acidophila* 10050 (two perpendicular views, A and B) and from *Phs. molischianum* LH2 (C and D, respectively) as search models. Cofactors in the *Phs. molischianum* LH2 were removed from the MR solution model (C and D) for clarity, due to rather poor electron density for them. The images were generated using the program COOT [43].

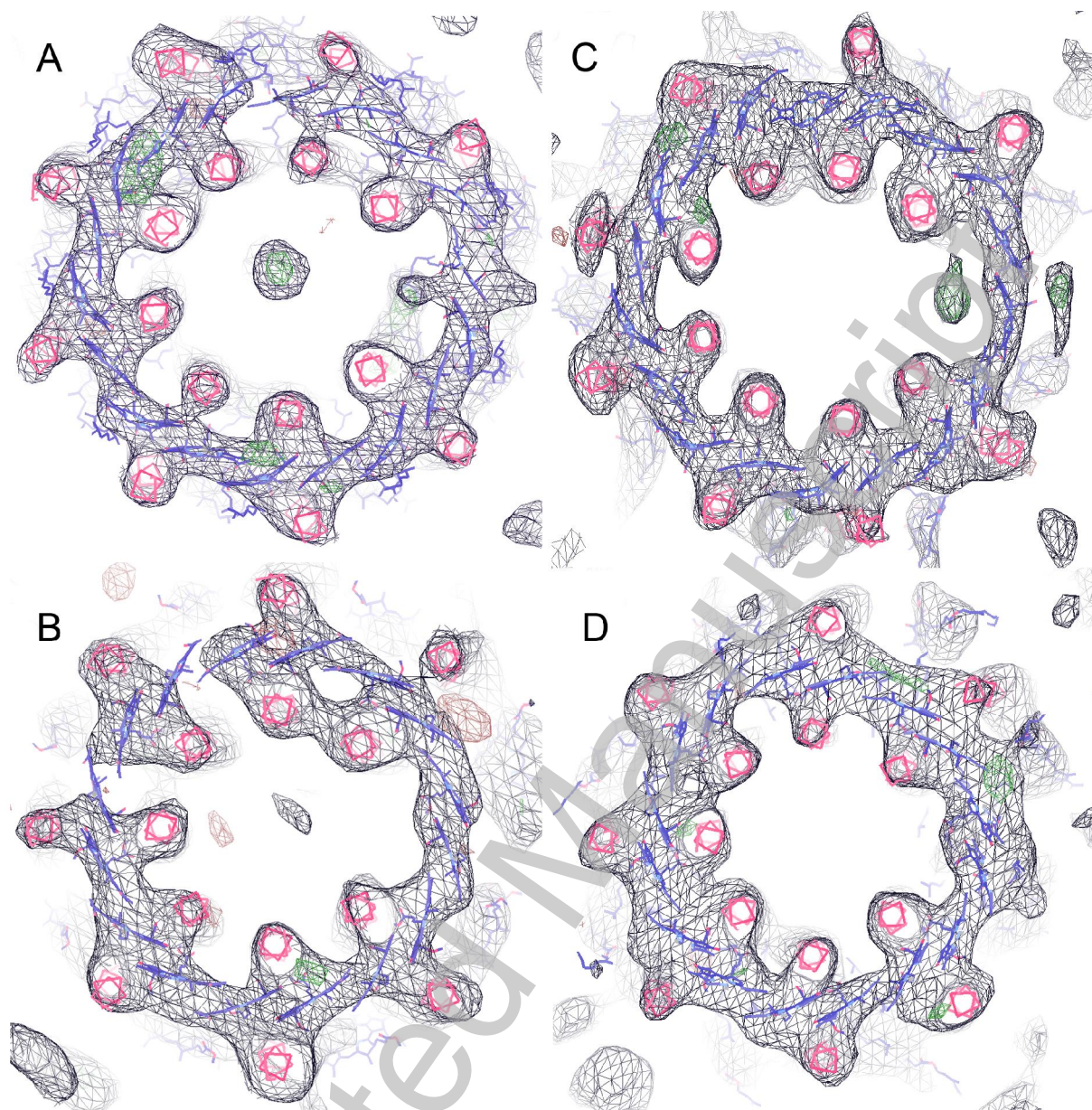


Figure 11. Omit maps calculated for the *Rps. palustris* LH2 molecular replacement models with one pair of the α/β -helices removed (at 3-o'clock position in each ring) for the jelly-body restrained refinement with program Refmac [33]. In each case the $2F_o-F_c$ electron density is shown at 1.0σ level in black and the F_o-F_c density is shown at 3.0σ level with the positive density in green and negative one in red/brown. The α/β -helices in the models are shown in red while the bacteriochlorophyll cofactors are shown in blue. (A) The HL-LH2 P_{21} -data and the *acidophila* LH2 model; (B) The HL-LH2 P_{21} -data and the *molischianum* LH2 model; (C) The LL-LH2 P_{21} -data and the *acidophila* LH2 model; (D) The HL-LH2 P_{21} -data and the *molischianum* LH2 model. The images were generated using the program COOT [35].